

# Bioinformatics analysis of the circRNA–miRNA–mRNA network for non-small cell lung cancer

Journal of International Medical Research  
48(6) 1–15

© The Author(s) 2020

Article reuse guidelines:

sagepub.com/journals-permissions

DOI: 10.1177/0300060520929167

journals.sagepub.com/home/imr



Xueying Cai<sup>1,\*</sup>, Lixuan Lin<sup>2,\*</sup>, Qiuhua Zhang<sup>3</sup>,  
Weixin Wu<sup>3,#</sup>  and An Su<sup>3,#</sup>

## Abstract

**Objective:** Non-small cell lung cancer (NSCLC) accounts for approximately 80% of all lung cancers, but its pathogenesis has not been fully elucidated. Therefore, it is valuable to explore the pathogenesis of NSCLC to improve diagnosis and identify novel treatment biomarkers.

**Methods:** Circular (circ)RNA, micro (mi)RNA, and gene expression datasets of NSCLC were analyzed to identify those that were differentially expressed between tumor and healthy tissues. Common genes were found and pathway enrichment analyses were performed. Survival analysis was used to identify hub genes, and their level of methylation and association with immune cell infiltration were analyzed. Finally, an NSCLC circRNA–miRNA–mRNA network was constructed.

**Results:** Eight miRNAs and 211 common genes were identified. Gene ontology and Kyoto Encyclopedia of Genes and Genomes analyses revealed that cell projection morphogenesis, blood vessel morphogenesis, muscle cell proliferation, and synapse organization were enriched. Ten hub genes were found, of which the expression of *DTL* and *RRM2* was significantly related to NSCLC patient prognosis. Significant methylation changes and immune cell infiltration correlations with *DTL* and *RRM2* were also detected.

**Conclusions:** hsa\_circ\_0001947/hsa-miR-637/RRM2 and hsa\_circ\_0072305/hsa-miR-127-5p/DTL networks were constructed, and identified molecules may be involved in the occurrence and development of NSCLC.

<sup>1</sup>Department of Respiratory Medicine, Zhongshan Hospital, Xiamen University, Xiamen City, Fujian Province, China

<sup>2</sup>Department of biotechnology, College of Life Sciences, Sichuan University, Chengdu, China

<sup>3</sup>Department of Internal Medicine and Oncology, Zhongshan Hospital, Xiamen University, Xiamen City, Fujian Province, China

\*These authors contributed equally to this work.

#These authors contributed equally to this work.

### Corresponding author:

Weixin Wu, Department of Internal Medicine and Oncology, Zhongshan Hospital, Xiamen University, 209 Hubin South Road, Siming District, Xiamen City, Fujian Province, 361000, China.

Email: wu3170536@sina.com



## Keywords

Non-small cell lung cancer, bioinformatics, hub gene, circular RNA, microRNA, differential expression, methylation, survival analysis

Date received: 17 January 2020; accepted: 1 May 2020

## Introduction

Non-small cell lung cancer (NSCLC) is the most common type of lung cancer, and NSCLC patients are prone to recurrence and have a poor prognosis.<sup>1</sup> Changes in social lifestyles and environments have led to increases in the incidence of NSCLC, with around 234,000 new cases reported in the United States each year.<sup>2</sup> NSCLC patients have no obvious symptoms in the early stage of disease, although they may experience chest pain, fever, and cough.<sup>3</sup> Indeed, the pathogenesis of NSCLC has not been fully elucidated. Many factors including smoking, the environment, inflammation, and genetics may be related to the development of tumors,<sup>4,5</sup> while small molecules such as circular (circ) RNAs and micro (mi)RNAs were also reported to be involved in tumor progression.<sup>6,7</sup> Additionally, treatment methods and effects correlate with tumor stage.<sup>8</sup> For patients in the early stages of disease, surgery is the first choice of treatment.<sup>8</sup> Radiotherapy, chemotherapy, and biotargeted therapy can be used in combination in advanced patients while avoiding unnecessary surgery.<sup>9</sup> However, the prognosis of patients is far from satisfactory because of the high tumor recurrence and metastasis rates.<sup>10,11</sup> Therefore, it is valuable to further explore the pathogenesis of NSCLC and identify targets to aid early diagnosis and the development of specific treatments.

Bioinformation technology can identify molecular markers related to tumor progression by analyzing tumor sequencing

data. Bai et al used weighted gene co-expression network analysis to identify multiple genes related to breast cancer subtypes, recognize key modules and hub genes, and prove that the tumor microenvironment and immune infiltration are involved in the occurrence and development of breast cancer.<sup>12</sup> Zhan et al found that CD276 regulates protein phosphorylation and thus participates in glioblastoma progression, suggesting that it could be used as a therapeutic biomarker for glioblastoma.<sup>13</sup> Additionally, Xiao et al analyzed circRNA and gene expression data to detect multiple molecules abnormally expressed in the pancreas of ductal adenocarcinoma patients, and constructed a circRNA–miRNA–mRNA network providing novel ideas for mechanism research and treatment.<sup>14</sup> Furthermore, Dai detected multiple genes that are abnormally expressed in patients with NSCLC and used bioinformatic analysis to identify hub genes as potential early diagnosis and treatment biomarkers.<sup>15</sup>

In the present study, we screened differentially expressed circRNAs (DECs), miRNAs (DEMs), and genes (DEGs) between NSCLC tumor tissues and healthy lung tissues by bioinformatic analysis. Our findings were used to construct a circRNA–miRNA–mRNA network of NSCLC.

## Materials and methods

### *NSCLC expression dataset*

The gene expression omnibus (GEO; <http://www.ncbi.nlm.nih.gov/geo>) is a public

platform for the storage of genetic data.<sup>16</sup> One circRNA expression profiling dataset [GSE112214 (GPL19978 platform)], one miRNA expression profiling dataset [GSE102286 (GPL23871 platform)], and one gene expression profiling dataset [GSE101929 (GPL570 platform)] were downloaded from the GEO database. The GSE112214 dataset includes three NSCLC lung samples and three matched adjacent healthy samples; GSE102286 includes 179 tumor and paired healthy tissues from African-Americans and European-Americans with NSCLC and we selected 10 paired tumor and healthy tissues from both ethnic groups; GSE101929 includes 66 tumor and paired healthy tissues from African-Americans and European-Americans with NSCLC and we again selected 10 from both ethnic groups.

### ***DEC, DEM, and DEG identification***

GEO2R (<https://www.ncbi.nlm.nih.gov/geo/geo2r/>) is an online tool used to identify DEGs in datasets from the GEO.<sup>17</sup> It may also be used to identify DEGs, DEMs, and DECs between NSCLC tumor and healthy tissue samples. We used it with statistical parameters: P-value <0.05 and fold change (FC) >1 or FC <-1 (GSE112214, GSE102286) or FC >2 or FC<-2 (GSE101929). Volcano diagrams were delineated by SangerBox software (<http://sangerbox.com/>), and circRNAs were analyzed in circBase (<http://www.circbase.org/>).

### ***miRNA and mRNA prediction***

The most 10 significantly changed DECs were used to predict downstream miRNAs through Circinteractome.<sup>18</sup> Additionally, intersection miRNAs of the predicted miRNAs and DEMs were used to predict downstream mRNAs through miRWalk 3.0.<sup>19</sup> Genes common to both predicted mRNAs and DEGs were identified.

Venn diagrams were delineated by FunRich software (<http://www.funrich.org>).

### ***KEGG and GO pathway enrichment analysis***

The Database for Annotation, Visualization and Integrated Discovery (DAVID) (<https://david.ncifcrf.gov/home.jsp>; version 6.8) is an online suite of analysis tools.<sup>20</sup> We used the DAVID online tool to perform Gene Ontology (GO) and Kyoto Encyclopedia of Genes and Genomes (KEGG) analysis of common genes, with P < 0.05 indicating statistical significance. The online tool Metascape (<http://metascape.org/gp/index.html>) was used to visualize pathway and process enrichment analyses.

### ***Protein-protein interaction (PPI) network analysis***

The PPI network was constructed by the online tool Search Tool for the Retrieval of Interacting Genes (<http://string.embl.de/>). Next, Cytoscape visualization software (version 3.6.1) was used to visualize the network.<sup>21</sup> The judgment criterion was set as score >0.4.

### ***Identification and analysis of hub genes***

Significant modules were identified by the Cytoscape plug-in Molecular Complex Detection with degree cut-off = 2 and Max depth = 100. Then, cytoHubba, a free plug-in was used to determine hub genes when degrees  $\geq 10$ .

### ***Expression analysis of hub genes and survival analysis***

UCSC Xena (<https://xena.ucsc.edu/wel-come-to-ucsc-xena/>) was used to integrate public genomic data sets to analyze and visualize gene expression in tumors. Then, clustering analysis of hub gene expression levels was performed by heatmaps.

GEPIA is an online tool for analyzing gene expression in cancer and healthy samples (<http://gepia.cancer-pku.cn/>),<sup>22</sup> which we used to analyze the following survival times: 50 months, 100 months, 150 months, 200 months, and 250 months. GEPIA was also used to analyze the expression of hub genes in different tumor stages of NSCLC, and to verify the expression levels of hub genes. The following settings were used: Expression on Box Plots [ $\text{Log}_2\text{FC}$ ] Cutoff = 1, p-value cutoff = 0.01, jitter size = 0.4, and match TCGA data.

### Candidate gene analysis

The methylation of candidate genes in NSCLC was assessed using DiseaseMeth version 2.0.<sup>23</sup> Additionally, the immune cell infiltration of candidate genes in NSCLC was analyzed by Tumor Immune Estimation Resource.<sup>24</sup>

### CircRNA–miRNA–mRNA network construction

The circRNA–miRNA–mRNA network was constructed using Cytoscape visualization software (version 3.6.1; <https://cytoscape.org/>) according to the interaction between circRNA, miRNA, and mRNA.

## Results

### Screening of DECs, DEMs, and DEGs between NSCLC tumor and healthy tissues

Volcano plots show DECs, DEMs, and DEGs (Figure 1a–c). The five most significantly upregulated (hsa\_circ\_0017956, hsa\_circ\_0001998, hsa\_circ\_0007580, hsa\_circ\_0017109, and hsa\_circ\_0006006) and downregulated (hsa\_circ\_0072309, hsa\_circ\_0008234, hsa\_circ\_0006677, hsa\_circ\_0001947, hsa\_circ\_0072305) circRNAs were chosen to predict miRNAs. Basic

information of these 10 differentially expressed circRNAs is shown in Table 1. Eight miRNAs (hsa-miR-598, hsa-miR-155, hsa-miR-644, hsa-miR-145, hsa-miR-637, hsa-miR-127-5p, hsa-miR-488, hsa-miR-369-5p) were found to be common between circRNA-predicted miRNAs and DEMs of dataset GSE102286 (Figure 1d). The 211 genes common to both the eight miRNA-predicted genes and DEGs of dataset GSE101929 are shown in a Venn diagram (Figure 1e).

### Pathway and process enrichment analysis

Enrichment analysis showed that variations were predominantly enriched in cell projection morphogenesis, blood vessel morphogenesis, muscle cell proliferation, synapse organization, regulation of the MAPK cascade, regulation of cell junction assembly, and DNA replication initiation. Pathway and process enrichment analyses findings by Metascape are shown in Figure 2a–c.

### PPI network and hub gene selection

The construction of a PPI network revealed 412 edges and 129 nodes (Figure 3a). The key module involved 21 nodes and 190 edges (Figure 3b). The top 10 hub genes were identified (*HMMR*, *MCM10*, *NUSAPI*, *PBK*, *RRM2*, *ASF1B*, *OIP5*, *CDC6*, *DTL*, and *FANCI*; Figure 3c).

### Hub gene analysis

Expression analysis in UCSC Xena showed that all 10 hub genes were highly expressed in NSCLC tumor tissues (Figure 3d). Survival analysis of the hub genes is shown in Figure 4a–j, and *DTL* and *RRM2* were found to be significantly associated with patient prognosis ( $P < 0.05$ ; Figure 4c, j) so were chosen as candidate genes. The correlation of hub genes and tumor stage is shown in Figure 5a–j, and

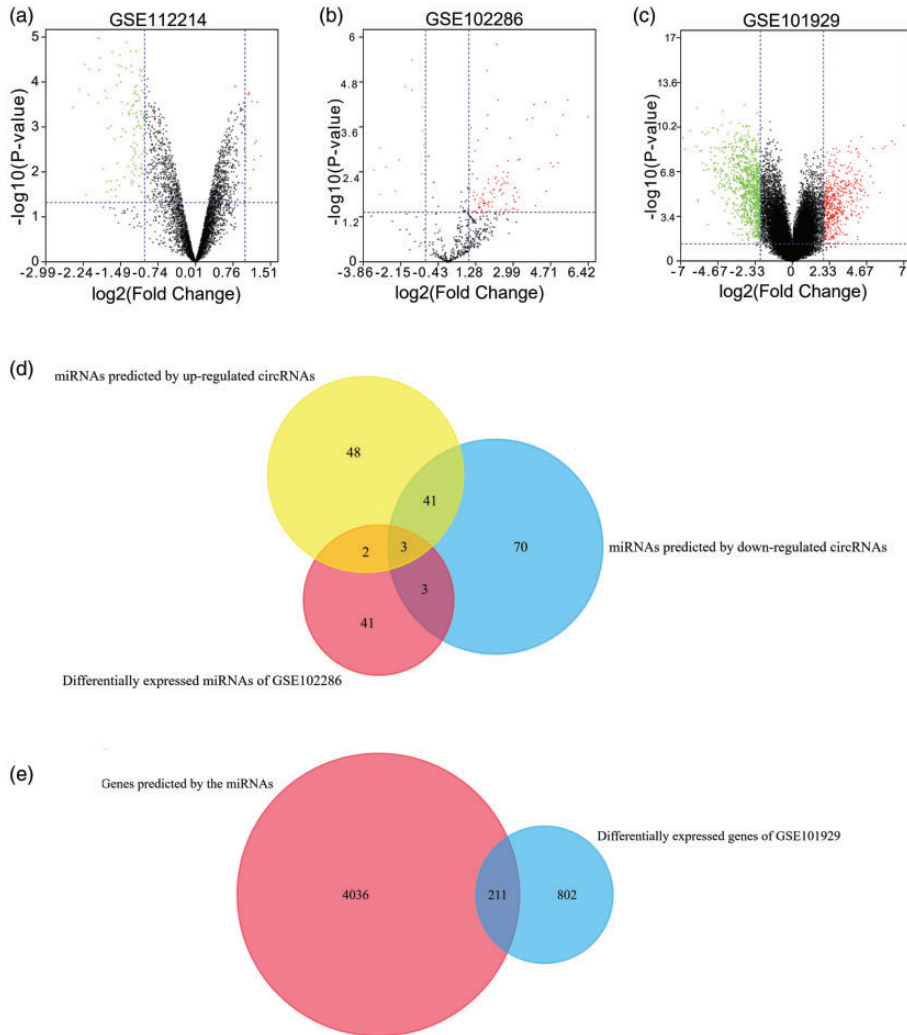


**Figure 1.** Identification of differentially expressed circRNAs (DECs), miRNAs (DEMs), and genes (DEGs). Volcano plots show DECs (a), DEMs (b), and DEGs (c).

suggested that these hub genes are involved in the occurrence and development of tumors and in promoting tumor progression. GEPIA analysis of hub gene expression in NSCLC is shown in Figure 6a–i.

### Candidate gene analysis

The methylation levels of both *DTL* (Figure 7a, b) and *RRM2* (Figure 7c, d) were lower in patients with lung adenocarcinoma and

lung squamous cell carcinoma than in healthy controls. Immune infiltration analysis revealed a significant correlation between the expression of *DTL* and *RRM2* and the abundance of immune infiltration in NSCLC (Figure 8a–d).

### Network construction

The circRNA–miRNA–mRNA network of NSCLC is shown in Figure 9a. Notably, the

**Table 1.** The top 10 most differentially expressed circRNAs.

CircRNA	Alias	Position	Gene symbol	Regulation
hsa_circRNA_100565	hsa_circ_0017956	chr10: 22019828-22024164	<i>MLL10</i>	Up
hsa_circRNA_101367	hsa_circ_0001998	chr14: 65922338-66028484	<i>FUT8</i>	Up
hsa_circRNA_102179	hsa_circ_0007580	chr17: 64728805-64738878	<i>PRKCA</i>	Up
hsa_circRNA_100498	hsa_circ_0017109	chr1: 236192849-236201553	<i>NIDI</i>	Up
hsa_circRNA_102856	hsa_circ_0006006	chr2: 173435453-173460751	<i>PDK1</i>	Up
hsa_circRNA_103820	hsa_circ_0072309	chr5: 38523520-38530768	<i>LIFR</i>	Down
hsa_circRNA_103415	hsa_circ_0008234	chr3: 71090478-71102924	<i>FOXP1</i>	Down
hsa_circRNA_100259	hsa_circ_0006677	chr1: 67356836-67371058	<i>WDR78</i>	Down
hsa_circRNA_105034	hsa_circ_0001947	chrX: 147743428-147744289	<i>AFF2</i>	Down
hsa_circRNA_103819	hsa_circ_0072305	chr5: 38496483-38530768	<i>LIFR</i>	Down

hsa\_circ\_0001947/hsa-miR-637/RRM2 and hsa\_circ\_0072305/hsa-miR-127-5p/DTL networks were found to be of interest and deserve further study (Figure 9b).

## Discussion

NSCLC includes squamous cell carcinoma, adenocarcinoma, and large cell carcinoma, and accounts for approximately 80% of all lung cancers.<sup>25</sup> Because many NSCLC patients are in the advanced stage of disease at the time of diagnosis and as tumors are prone to recurrence, the patient 5-year survival rate is far from satisfactory.<sup>2</sup> Surgical resection is most effective for patients with early-stage disease, while chemotherapy and bio-targeted therapy are recommended for those at middle and advanced stages.<sup>8,26</sup> Mitchell et al. identified multiple differentially expressed molecules in African-American and European-American patients with NSCLC through genetic and miRNA sequencing. They also used functional enrichment analysis and tumor immune microenvironment analysis to investigate the mechanism of NSCLC and the potential of immunotherapy.<sup>27</sup>

In the present study, multiple differentially expressed molecules were found from the sequencing data of circRNAs, miRNAs, and mRNAs in NSCLC through bioinformatic analysis. CircRNAs most

significantly altered in expression were used to predict relevant miRNAs, and the intersection of predicted miRNAs and DEMs calculated by datasets was determined. Furthermore, intersection miRNAs were successfully used to predict related mRNAs, and multiple genes common to these mRNAs and DEGs were identified. GO and KEGG analyses of common intersection genes enabled the construction of a PPI network and identification of hub genes (*HMMR*, *MCM10*, *NUSAPI*, *PBK*, *RRM2*, *ASF1B*, *OIP5*, *CDC6*, *DTL*, and *FANCI*) most likely to participate in NSCLC from the intersection genes. Finally, we constructed the circRNA-miRNA-mRNA network and identified regulatory molecule networks hsa\_circ\_0001947/hsa-miR-637/RRM2 and hsa\_circ\_0072305/hsa-miR-127-5p/DTL as potentially playing important roles in the occurrence and development of NSCLC. Candidate gene analysis involving an assessment of gene methylation levels and survival analysis of NSCLC data in the TCGA database identified *RRM2* and *DTL* as having lower methylation in NSCLC patients than healthy controls, and being significantly correlated in expression levels with the abundance of immune infiltration in NSCLC.

*RRM2* encodes ribonucleotide reductase regulatory subunit M2, which regulates

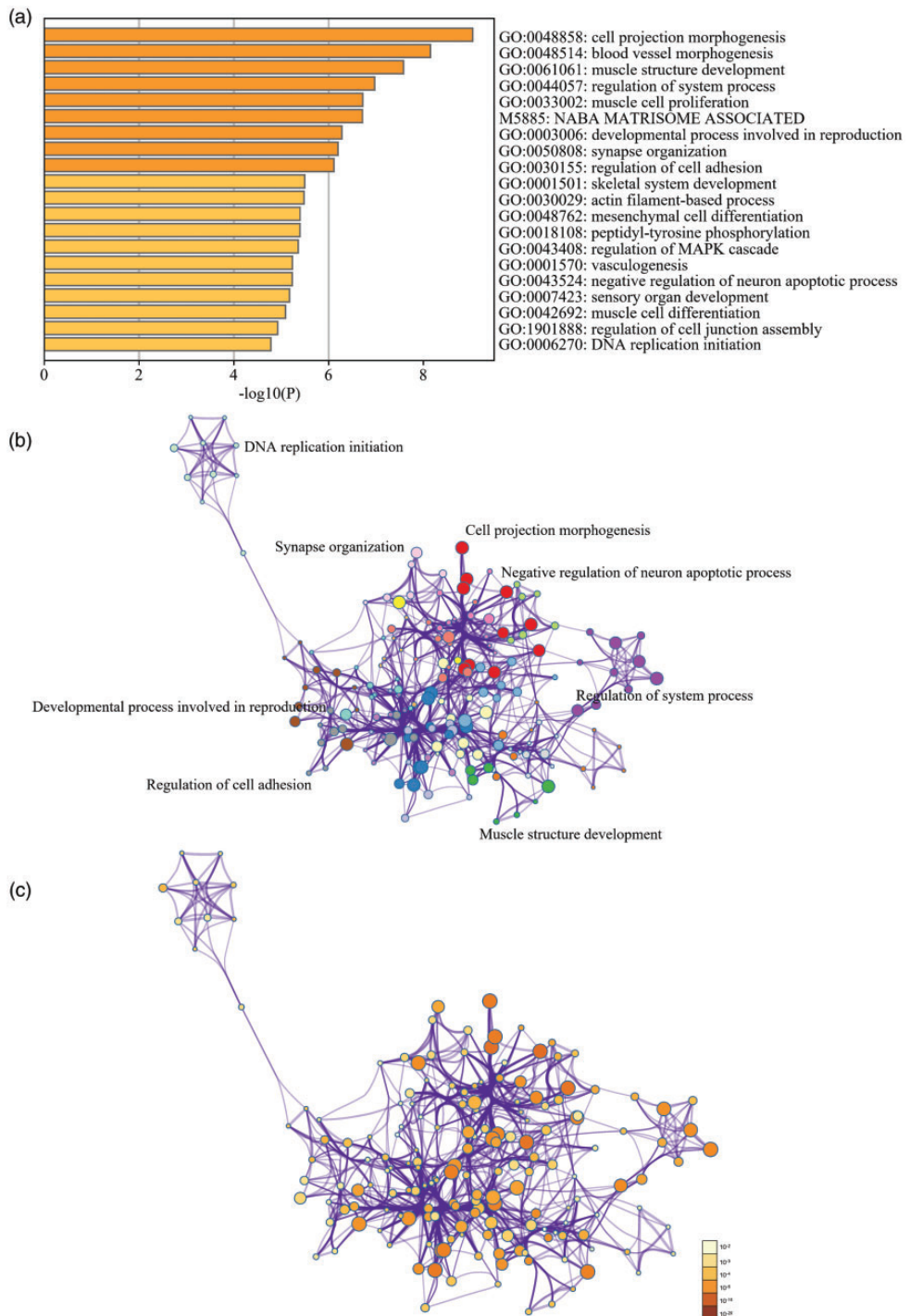


**Figure 2.** Network of enriched terms. (a) Pathway and process enrichment analysis colored by cluster ID (b) and p-value (c).

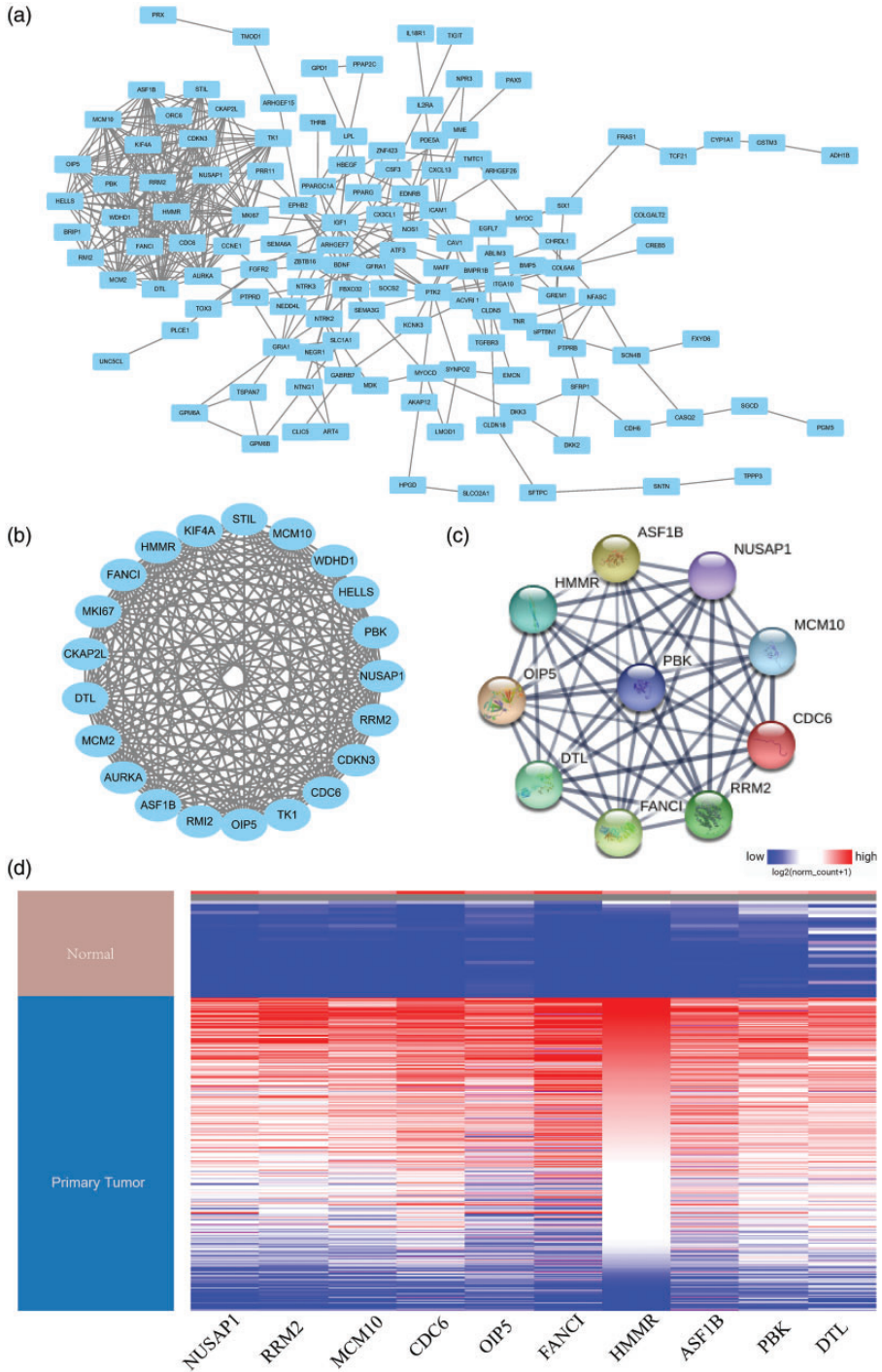


**Figure 3.** PPI network and expression analysis. (a) Protein–protein interaction (PPI) network of common genes, consisting of 412 edges and 129 nodes. (b) The most important module of the network map. (c) Hub genes identified within the PPI network. (d) Expression analysis in UCSC.



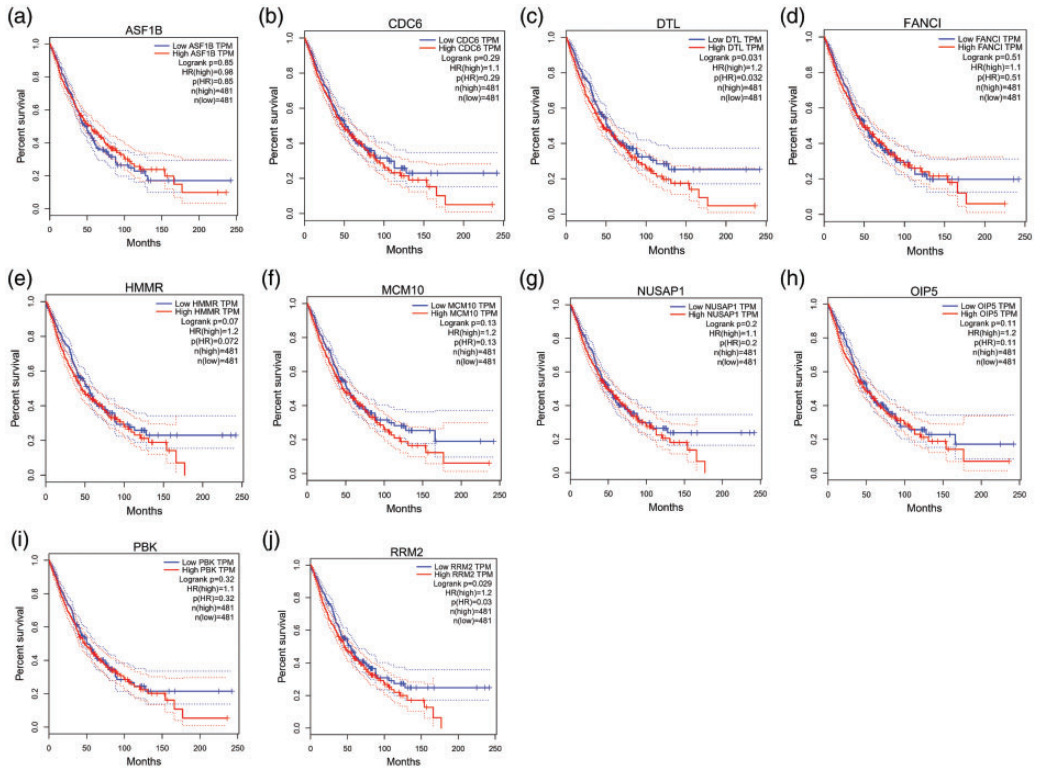


**Figure 4.** Survival analysis of hub genes. (a) *ASF1B*, (b) *CDC6*, (c) *DTL*, (d) *FANCI*, (e) *HMMR*, (f) *MCM10*, (g) *NUSAP1*, (h) *OIP5*, (i) *PBK*, and (j) *RRM2*.

ribonucleoside-diphosphate reductase activity, protein binding, and transcription in G1/S transition of the mitotic cell cycle, as well as DNA replication, oxidation-reduction, and G0 to G1 transition. The abnormal expression of *RRM2* is seen in the occurrence and development of several diseases. Altinkilic et al found that *RRM2* may participate in the occurrence and development of atherosclerotic plaques in the coronary arteries by regulating DNA damage repair.<sup>28</sup> Zhong et al showed that *RRM2* is highly expressed in gastric cancer tissues, and that it may affect the proliferation and migration of gastric cancer cells by regulating AKT and nuclear factor- $\kappa$ B signaling pathways, suggesting that it could be used as a target for early diagnosis and treatment of gastric cancer.<sup>29</sup> Additionally,

Castelblanco et al constructed a predictive model showing that *RRM2* can be used to distinguish thyroid tumors from benign lesions, and providing new insights for the early diagnosis and treatment of thyroid tumors.<sup>30</sup> Similarly, Li et al reported that *RRM2* participates in the occurrence and development of glioblastoma by regulating cell apoptosis, proliferation, and migration, indicating its potential as a therapeutic target.<sup>31</sup> Furthermore, Yang et al found that *RRM2* is regulated by LINC00667/miR-143-3p and that it may affect the proliferation of NSCLC cells, thus affecting the prognosis of patients and suggesting that related molecules may be used as treatment targets.<sup>32</sup> Here, we observed that *RRM2* is highly expressed in NSCLC patients, and survival analysis revealed a correlation

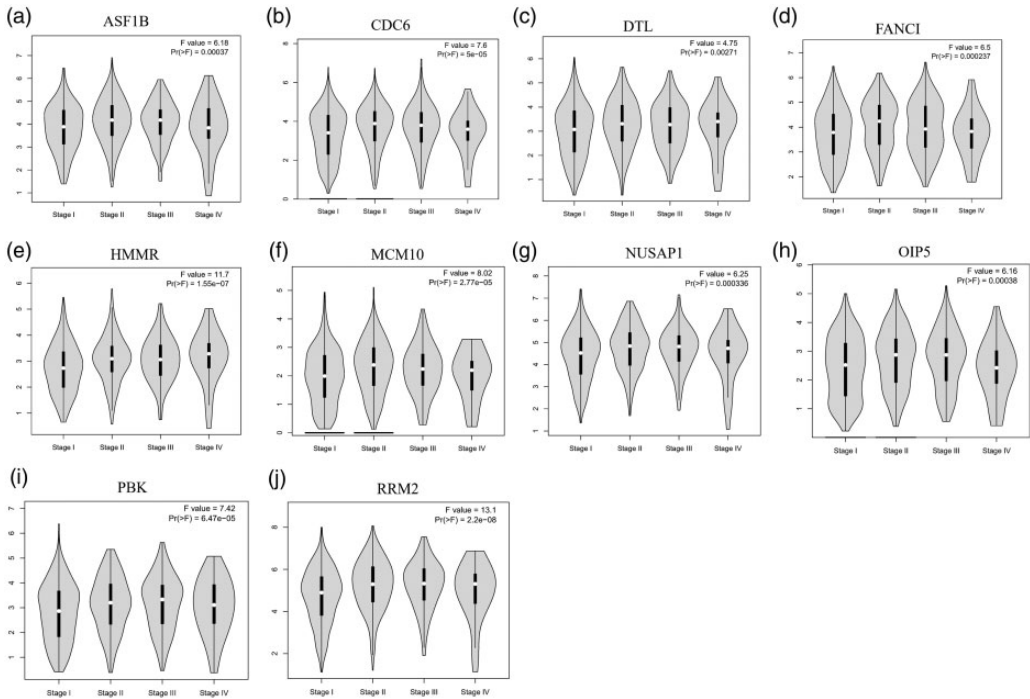


**Figure 5.** The correlation of hub genes and the tumor stage. (a) *ASF1B*, (b) *CDC6*, (c) *DTL*, (d) *FANCI*, (e) *HMMR*, (f) *MCM10*, (g) *NUSAP1*, (h) *OIP5*, (i) *PBK*, and (j) *RRM2*.

between high expression and poor prognosis. We also detected significant *RRM2* methylation changes in patients with NSCLC, and a significant correlation between *RRM2* expression and multiple immune infiltrations was found. We speculate that *RRM2* participates in the occurrence and development of NSCLC by regulating the cell cycle, apoptosis, and inflammation levels. The hsa\_circ\_0001947/hsa-miR-637/*RRM2* network may serve as a target for the early diagnosis and specific treatment of NSCLC, and the related regulatory mechanism deserves further study.

*DTL* encodes denticleless E3 ubiquitin protein ligase homolog, which is mainly involved in the regulation of ubiquitin-protein transferase activity, protein polyubiquitination, DNA replication, and G2/M transition of the mitotic cell cycle. The abnormal expression of *DTL* is involved

in the occurrence and development of various diseases. Baraniskin et al found that miR-30a-5p affected the cell cycle and apoptosis of colon cancer cells by regulating the expression of *DTL*,<sup>33</sup> while Perez et al detected abnormal *DTL* expression in patients with breast cancer which was associated with poor prognosis. Further analysis found that *DTL* may affect the sensitivity of tumor cells to drugs by regulating protein ubiquitination.<sup>34</sup> Additionally, Cui et al demonstrated that *DTL* may affect the apoptosis and proliferation of tumor cells by regulating the ubiquitination degradation of programmed cell death.<sup>35</sup> Thus, *DTL* could serve as a target biomarker for the immunotherapy of various tumors, offering new clues for tumor immunotherapy. Similar to this research, we found that *DTL* was highly expressed in NSCLC patients, and survival analysis found that

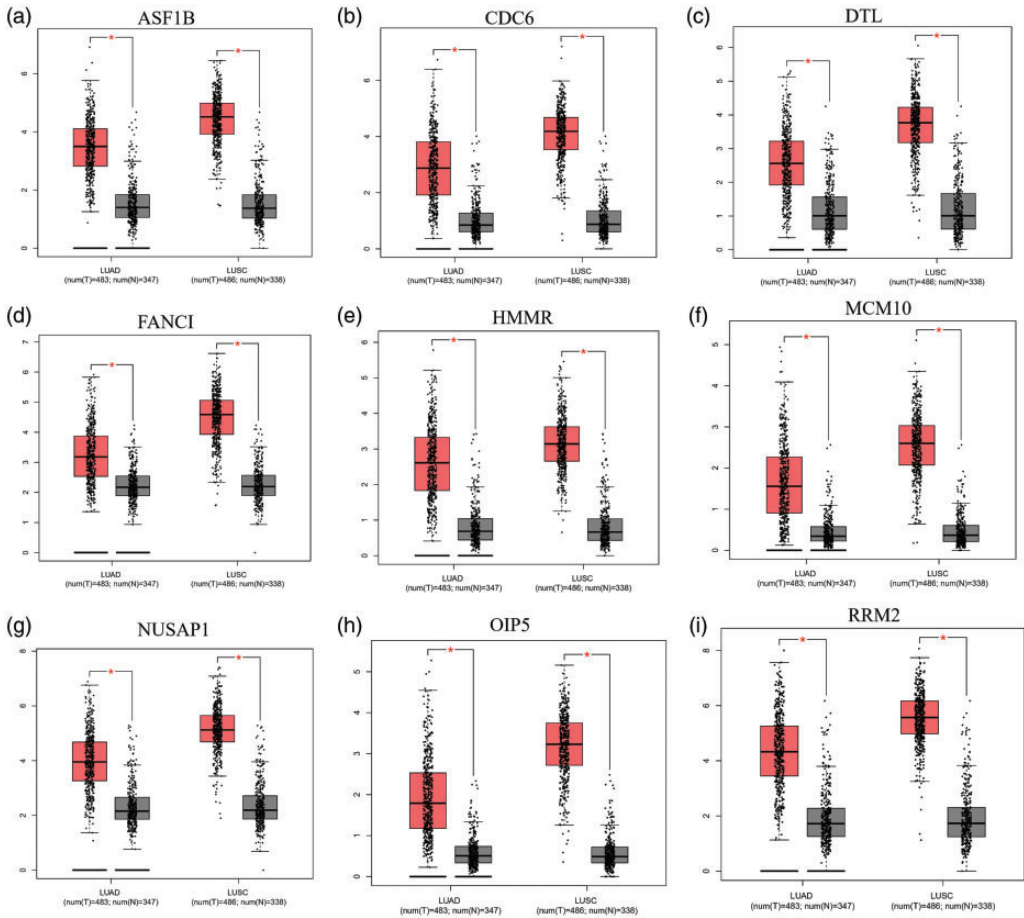


**Figure 6.** Relative expression of the hub gene in NSCLC in GEPIA. (a) *ASF1B*, (b) *CDC6*, (c) *DTL*, (d) *FANCI*, (e) *HMMR*, (f) *MCM10*, (g) *NUSAP1*, (h) *OIP5*, and (i) *RRM2*.

high expression was associated with poor prognosis. Furthermore, we detected significant *DTL* methylation changes in patients with NSCLC, and found a correlation between *DTL* expression and multiple immune infiltrations. We speculate that *DTL* may also participate in the occurrence and development of NSCLC by regulating the cell cycle, apoptosis, and cellular information conduction. The *hsa\_circ\_0072305/hsa-miR-127-5p/DTL* network could also serve as a target for the early diagnosis and specific treatment of NSCLC, and the

related regulatory mechanism deserves further exploration.

Despite the rigorous bioinformatics analysis of this study, there are still some shortcomings. First, the sample size in the dataset was small, so should be further expanded to obtain more accurate results. Second, functional verification experiments need to be performed.

In conclusion, bioinformatics analysis appears to be a useful tool to explore the pathogenesis and therapeutic targets of NSCLC. We successfully constructed a circRNA–miRNA–mRNA network of

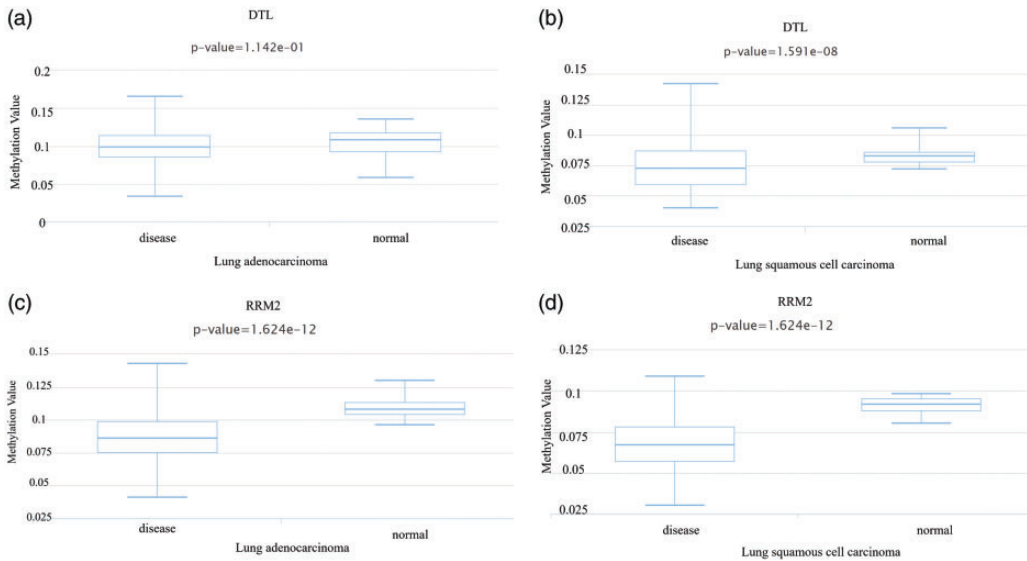


**Figure 7.** The methylation level of *DTL* and *RRM2* in patients with lung adenocarcinoma and lung squamous cell carcinoma. (a, b) *DTL* and (c, d) *RRM2*.

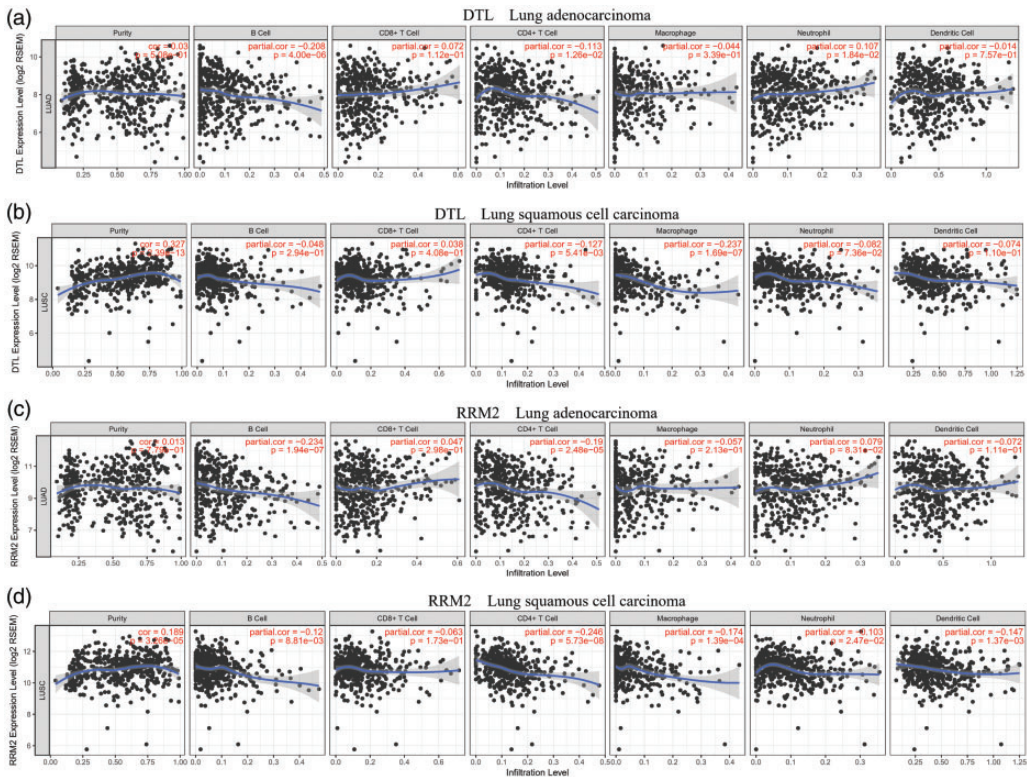


**Figure 8.** Correlation analysis of hub gene expression and immune infiltration. (a, b) *DTL* and (c, d) *RRM2*.

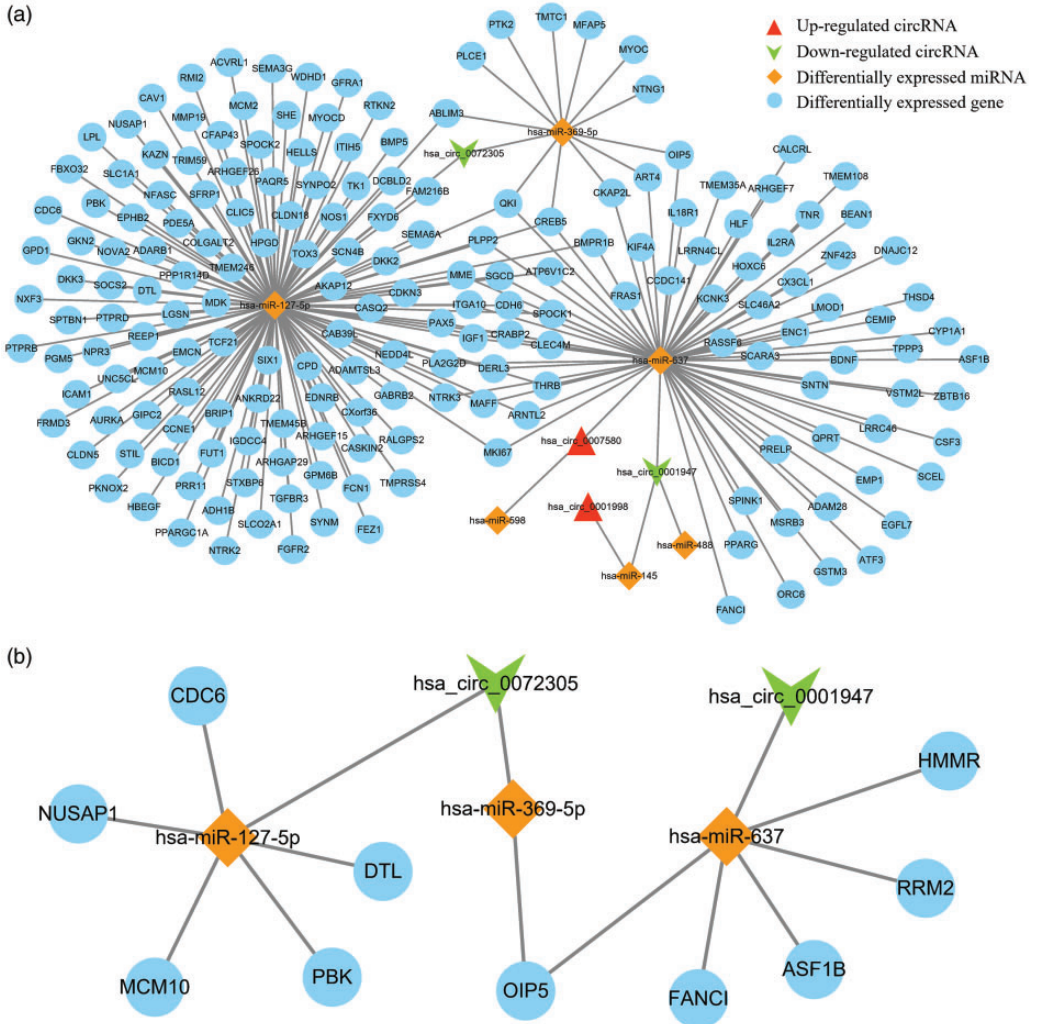


**Figure 9.** The circRNA–miRNA–mRNA network. (a) All related molecules. (b) The hub genes most significantly associated with miRNAs and circRNAs.

NSCLC, and the identified molecules may be involved in the occurrence and development of NSCLC so could serve as molecular targets for early diagnosis and specific treatment.

**Author contributions**

Xueying Cai and Lixuan Lin performed the experiments and were major contributors in writing and submitting the manuscript. Weixin

Wu and An Su made substantial contributions to research conception and designed the research process. Qihua Zhang, Xueying Cai, and Lixuan Lin critically revised the manuscript for important intellectual content. All authors read and approved the final manuscript.

**Acknowledgements**

We are thankful to Chen Xi for her suggestions during the submitting process.

### Availability of data and materials

The datasets used and/or analyzed during the current study are available from the corresponding author on reasonable request.

### Declaration of conflicting interest

The authors declare that there is no conflict of interest.


### Ethics approval and consent to participate

The data of this research were downloaded from the GEO database. All institutional and national guidelines for the care and use of participants were followed.

### Funding

This research received no specific grant from any funding agency in the public, commercial, or not-for-profit sectors.

### ORCID iD

Weixin Wu  <https://orcid.org/0000-0003-3062-6787>

### Patient consent for publication

Not applicable.

### References

- Guerrera F, Errico L, Evangelista A, et al. Exploring Stage I non-small-cell lung cancer: development of a prognostic model predicting 5-year survival after surgical resection. *Eur J Cardiothorac Surg* 2015; 47: 1037–1043.
- Siegel RL, Miller KD, Jemal A, et al. Cancer statistics, 2018. *CA Cancer J Clin* 2018; 68: 7–30.
- Xing PY, Zhu YX, Wang L, et al. What are the clinical symptoms and physical signs for non-small cell lung cancer before diagnosis is made? A nation-wide multicenter 10-year retrospective study in China. *Cancer Med* 2019; 8: 4055–4069.
- Qin A, Coffey DG, Warren EH, et al. Mechanisms of immune evasion and current status of checkpoint inhibitors in non-small cell lung cancer. *Cancer Med* 2016; 5: 2567–2578.
- Jacobsen K, Bertran-Alamillo J, Molina MA, et al. Convergent Akt activation drives acquired EGFR inhibitor resistance in lung cancer. *Nat Commun* 2017; 8: 410.
- Li C, Zhang L, Meng G, et al. Circular RNAs: pivotal molecular regulators and novel diagnostic and prognostic biomarkers in non-small cell lung cancer. *J Cancer Res Clin Oncol* 2019; 145: 2875–2889.
- Iqbal MA, Arora S, Prakasam G, et al. MicroRNA in lung cancer: role, mechanisms, pathways and therapeutic relevance. *Mol Aspects Med* 2019; 70: 3–20.
- Arbour KC and Riely GJ. Systemic therapy for locally advanced and metastatic non-small cell lung cancer: a Review. *JAMA* 2019; 322: 764–774.
- Forde PM, Chaft JE, Smith KN, et al. Neoadjuvant PD-1 blockade in resectable lung cancer. *N Engl J Med* 2018; 378: 1976–1986.
- Ostheimer C, Evers C, Palm F, et al. Mortality after radiotherapy or surgery in the treatment of early stage non-small-cell lung cancer: a population-based study on recent developments. *J Cancer Res Clin Oncol* 2019; 145: 2813–2822.
- Yang CJ, Kumar A, Klapper JA, et al. A national analysis of long-term survival following thorascopic versus open lobectomy for stage I non-small cell lung cancer. *Ann Surg* 2019; 269: 163–171.
- Bai F, Jin Y, Zhang P, et al. Bioinformatic profiling of prognosis-related genes in the breast cancer immune microenvironment. *Aging (Albany NY)* 2019; 11: 9328–9347.
- Zhang J, Wang J, Marzese DM, et al. B7H3 regulates differentiation and serves as a potential biomarker and theranostic target for human glioblastoma. *Lab Invest* 2019; 99: 1117–1129.
- Xiao Y. Construction of a circRNA-miRNA-mRNA network to explore the pathogenesis and treatment of pancreatic ductal adenocarcinoma. *J Cell Biochem* 2020; 121: 394–406.
- Dai B, Ren LQ, Han XY, et al. Bioinformatics analysis reveals 6 key biomarkers associated with non-small-cell lung

- cancer. *J Int Med Res* 2019. DOI: 10.1177/0300060519887637.
16. Edgar R, Domrachev M and Lash AE. Gene Expression Omnibus: NCBI gene expression and hybridization array data repository. *Nucleic Acids Res* 2002; 30: 207–210.
  17. Barrett T, Wilhite SE, Ledoux P, et al. NCBI GEO: archive for functional genomics data sets—update. *Nucleic Acids Res* 2013; 41: D991–D995.
  18. Dudekula DB, Panda AC, Grammatikakis I, et al. CircInteractome: a web tool for exploring circular RNAs and their interacting proteins and microRNAs. *RNA Biol* 2016; 13: 34–42.
  19. Sticht C, De La Torre C, Parveen A, et al. miRWalk: an online resource for prediction of microRNA binding sites. *PLoS One* 2018; 13: e0206239.
  20. Huang DW, Sherman BT, Tan Q, et al. The DAVID gene functional classification tool: a novel biological module-centric algorithm to functionally analyze large gene lists. *Genome Biol* 2007; 8: R183.
  21. Smoot ME, Ono K, Ruscheinski J, et al. Cytoscape 2.8: new features for data integration and network visualization. *Bioinformatics* 2011; 27: 431–432.
  22. Tang Z, Li C, Kang B, et al. GEPIA: a web server for cancer and normal gene expression profiling and interactive analyses. *Nucleic Acids Res* 2017; 45: W98–W102.
  23. Xiong Y, Wei Y, Gu Y, et al. DiseaseMeth version 2.0: a major expansion and update of the human disease methylation database. *Nucleic Acids Res* 2017; 45: D888–D895.
  24. Li T, Fan J, Wang B, et al. TIMER: a web server for comprehensive analysis of tumor-infiltrating immune cells. *Cancer Res* 2017; 77: e108–e110.
  25. Wang BY, Huang JY, Chen HC, et al. The comparison between adenocarcinoma and squamous cell carcinoma in lung cancer patients. *J Cancer Res Clin Oncol* 2020; 146: 43–52.
  26. Hellmann MD, Paz-Ares L, Bernabe Caro R, et al. Nivolumab plus ipilimumab in advanced non-small cell lung cancer. *N Engl J Med* 2019; 381: 2020–2031.
  27. Mitchell KA, Zingone A, Toulabi L, et al. Comparative transcriptome profiling reveals coding and noncoding RNA differences in NSCLC from African Americans and European Americans. *Clin Cancer Res* 2017; 23: 7412–7425.
  28. Altinkilic EM, Isbir S, Gormus U, et al. RRM1, RRM2 and ERCC2 gene polymorphisms in coronary artery disease. *In Vivo* 2016; 30: 611–615.
  29. Zhong Z, Cao Y, Yang S, et al. Overexpression of RRM2 in gastric cancer cell promotes their invasiveness via AKT/NF-kappaB signaling pathway. *Pharmazie* 2016; 71: 280–284.
  30. Castelblanco E, Zafon C, Maravall J, et al. APLP2, RRM2, and PRC1: new putative markers for the differential diagnosis of thyroid follicular lesions. *Thyroid* 2017; 27: 59–66.
  31. Li C, Zheng J, Chen S, et al. RRM2 promotes the progression of human glioblastoma. *J Cell Physiol* 2018; 233: 6759–6767.
  32. Yang Y, Li S, Cao J, et al. RRM2 regulated by LINC00667/miR-143-3p signal is responsible for non-small cell lung cancer cell progression. *Oncotargets Ther* 2019; 12: 9927–9939.
  33. Baraniskin A, Birkenkamp-Demtroder K, Maghnoouj A, et al. MiR-30a-5p suppresses tumor growth in colon carcinoma by targeting DTL. *Carcinogenesis* 2012; 33: 732–739.
  34. Perez-Pena J, Corrales-Sanchez V, Amir E, et al. Ubiquitin-conjugating enzyme E2T (UBE2T) and denticleless protein homolog (DTL) are linked to poor outcome in breast and lung cancers. *Sci Rep* 2017; 7: 17530.
  35. Cui H, Wang Q, Lei Z, et al. DTL promotes cancer progression by PDCD4 ubiquitin-dependent degradation. *J Exp Clin Cancer Res* 2019; 38: 350.